

Living Anionic Surface-Initiated Polymerization (LASIP) of Styrene from Clay Nanoparticles Using Surface Bound 1,1-Diphenylethylene (DPE) Initiators

Xiaowu Fan,[†] Qingye Zhou,[‡] Chuanjun Xia,[‡] Walter Cristofoli,[‡]
Jimmy Mays,^{*,†,§} and Rigoberto Advincula^{*,†,‡}

Tri-campus Materials Science Program and Department of Chemistry, University of Alabama at Birmingham, Birmingham, Alabama 35294-1240, and Department of Chemistry, University of Tennessee, Knoxville, Tennessee 37996-1600

Received January 19, 2002. In Final Form: March 28, 2002

Nanocomposite materials of clay nanoparticles and polystyrene were prepared using living anionic surface-initiated polymerization (LASIP). The montmorillonite clay surface and intergallery interfaces were intercalated with 1,1-diphenylethylene (DPE), an organic cation and initiator derivative for anionic polymerization. Its intercalation was confirmed by a series of characterization methods including X-ray diffraction (XRD), FT-IR spectroscopy, thermogravimetric analysis (TGA), and X-ray photoelectron spectroscopy (XPS). The results showed a complete replacement of the Na counterions by the charged initiators. LASIP was performed in a high-vacuum reaction setup for anionic polymerization using different styrene monomer/initiator ratios. A living anionic polymerization mechanism was determined from molecular weight (MW) data and the molecular weight distribution. A comparison of FT-IR, TGA, XPS, XRD, and atomic force microscopy (AFM) data confirmed that polystyrene was indeed “grafted from” clay surfaces for these composite materials. The initiation efficiency was distinguished between surface- and intergallery interface-bound initiators.

Introduction

Polymer–clay nanocomposite materials are of fundamental and practical importance especially in applications requiring high barrier properties, high temperatures, and mechanical strength combined with polymer processability.¹ They have been prepared using a number of methods primarily, by the blending of polymers with clays and the polymerization of monomers in the presence of clay particles.^{1,2} For obvious reasons, the in situ attachment of polymers directly onto clay particles has the advantage of yielding composites that are more thermodynamically stable and have better aging properties.^{1,3,8,13} The synthesis of polymer–clay nanocomposites by in situ polymerization involves intercalative polymerization occurring inside the host galleries of clay particle lamellae and surfaces.³ Layered clays, e.g. montmorillonite aluminosilicates, contain metal cations such as Na⁺, Li⁺, and Ca²⁺ between layers that can be replaced by ion exchange. This means that positively charged organic initiators can replace the metal ions in the interlayer galleries, forming intercalated clay–organic initiator complexes.³ This initiator intercalation process plays a very crucial role in the whole synthetic scheme. First, the inserted organic cation provides the initiation functionality for polymerization.

Second, the tethered organic initiator improves the organophilicity of the silicate clay, thereby increasing the homogeneity of the clay–monomer–organic solvent system for polymerization. The significance of in situ polymerization after intercalation is based on the assumption that, as the polymer chain grows, the silicate layers become exfoliated to discrete lathes, forming a well-dispersed composite material. This in situ polymerization process can be categorized as a surface-initiated polymerization (SIP) scheme because it is initiated by a surface- or interface-bound initiator. In this case, the polymer is “grafted from” the surface and is confined by the environment and mechanism of a polymerization process at an interface. SIPs by free-radical,⁴ atomic-transfer polymerization (ATRP),⁵ 2,2,6,6-tetramethyl-1-piperidyloxy (TEMPO),⁶ cationic polymerization,⁷ and anionic polymerization^{8,9} have been reported on both high-surface-area particles and flat substrates. Recently, polymer–clay nanocomposites have been synthesized by anchoring a living free-radical polymerization initiator into the galleries of layered silicates with subsequent in situ polymerization or SIP.^{3a}

Living anionic polymerization is an excellent method for preparing near monodisperse homopolymers.^{10,11} It has been the method of choice for preparing a variety of block

* To whom correspondence should be addressed.

[†] Tri-campus Materials Science Program, University of Alabama at Birmingham.

[‡] Department of Chemistry, University of Alabama at Birmingham.

[§] University of Tennessee and Oak Ridge National Laboratory.

(1) Krishnamoorti, R.; Vaia, R. *Polymer Nanocomposites*; ACS Symposium Series 804; American Chemical Society: Washington, DC, 2002.

(2) (a) Pinnavaia, T. J.; Beall, G. Eds. *Polymer–Clay Nanocomposites*; Wiley: New York, 2000. (b) LeBaron, P.; Wang, Z.; Pinnavaia, T. J. *Appl. Clay Sci.* **1999**, *15*, 11.

(3) (a) Weimer, W.; Chen, H.; Giannelis, E.; Sogah, D. *J. Am. Chem. Soc.* **1999**, *121*, 1615. (b) Meier, L. P.; Shelden, R. A.; Caseri, W. R.; Suter, U. W. *Macromolecules* **1994**, *27*, 1637. (c) Giannelis, E. P.; Krishnamoorti, R.; Manias, E. *Adv. Polym. Sci.* **1999**, *138*, 108.

(4) Prucker, O.; Ruhe, J. *Macromolecules* **1998**, *31*, 602.

(5) Ejaz, M.; Yamamoto, S.; Ohno, K.; Tsujii, U.; Fukuda, T. *Macromolecules* **1998**, *31*, 5934.

(6) Husseman, M.; Malmstrom, E.; McNamara, M.; Mate, M.; Mecerreyes, D.; Benoit, D.; Hedrick, J.; Mansky, P.; Huang, E.; Russell, T.; Hawker, C. *Macromolecules* **1999**, *32*, 1424.

(7) Jordan, R.; Ulman, A. *J. Am. Chem. Soc.* **1998**, *120*, 243.

(8) (a) Zhou, Q.; Nakamura, Y.; Inaoka, S.; Park, M.; Wang, Y.; Mays, J.; Advincula, R. *PMSE Prepr. (ACS)* **1999**, *82*, 290. (b) Zhou, Q.; Nakamura, Y.; Inaoka, S.; Park, M.; Wang, Y.; Fan, X.; Mays, J.; Advincula, R. In *Polymer Nanocomposites*; Krishnamoorti, R., Vaia, R., Eds.; Oxford University Press: New York, 2002; p 39.

(9) (a) Jordan, R.; Ulman, A.; Kang, J.; Rafailovich, M.; Sokolov, J. *J. Am. Chem. Soc.* **1999**, *121*, 1016. (b) Quirk, R.; Mathers, R. *Polym. Bull.* **2001**, *6*, 471. (c) Tsubokawa, N.; Yoshihara, T.; Sone, Y. *Colloid Polym. Sci.* **1991**, *269*, 324.

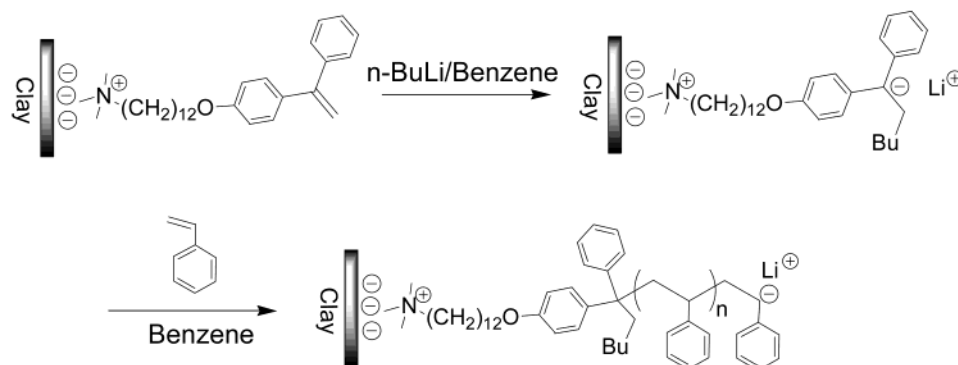


Figure 1. Schematic illustration of living anionic surface-initiated polymerization (LASIP) from clay surfaces.

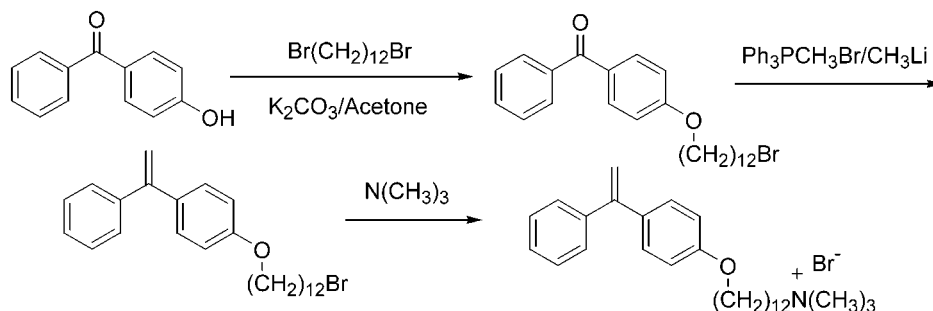


Figure 2. Synthetic scheme of the cationic (charged) 1,1-diphenylethylene (DPE) derivative initiator.

and complex graft copolymer architectures.¹² Anionic surface-initiated polymerization schemes have been reported on flat surfaces and particles.^{8,9} However, anionic SIP directly from clay particles is difficult, because the hydrophilic lamellar hosts inevitably contain moisture, which can terminate a propagating living anion.^{13,14} Nevertheless, we have demonstrated recently that, by using a 1,1-diphenylethylene (DPE) derivative as the initiator and carefully controlling the polymerization conditions, SIP from silicate clay surfaces is feasible.¹⁵ The DPE derivative was selected because it has high temperature stability and allows self-polymerization to be avoided.¹⁶ As shown in Figure 1, the quaternized-amine-modified DPE derivative can be immobilized on clay surfaces primarily by electrostatic attraction upon ion exchange. After being dispersed in benzene, the initiator–clay complex can be activated by *n*-BuLi to polymerize monomers.

In this paper, we describe in detail the procedure, conditions, and issues that concern a living anionic surface-initiated polymerization (LASIP) on montmorillonite clay nanoparticles intercalated with a DPE initiator derivative. The DPE initiator derivative was synthesized first. Its intercalation into clay nanoparticles by a stirring and ultrasonication process was confirmed by X-ray diffraction (XRD), FT-IR spectroscopy, thermogravimetric analysis (TGA), and X-ray photoelectron spectroscopy (XPS), all of which indicated complete replacement of the clay counterions by the charged initiators. LASIP was performed

in a special high-vacuum reaction setup for anionic polymerization with different styrene monomer/initiator ratios. Observations on the initiation process and molecular weight data of the detached polymer indicate that SIP was realized via a *living anionic* mechanism. A comparison of FT-IR, TGA, XPS, and XRD data confirmed the grafting of polystyrene from clay surfaces. In addition, atomic force microscopy (AFM) confirmed the initiation/chain growth efficiency differences between the clay nanoparticle surface perimeter and the lamellar interface.

Experimental Section

Materials. Montmorillonite clay (commercially known as Cloisite Na⁺) was provided by Southern Clay Products Co. (Gonzales, TX). Benzene (Fisher, >99%) was purified by stirring over concentrated sulfuric acid for 2 weeks, followed by overnight drying with ground calcium hydride (CaH₂) on a vacuum line and distillation. Styrene monomer (Aldrich, 99%) was dried over CaH₂, distilled from dibutylmagnesium (MgBu₂, Aldrich, 1.0 M in heptane), and collected in ampules using a short-path distillation apparatus. All other reagents were purchased from Aldrich and used without further purification.

Synthesis of the DPE Derivative. 1,1-Diphenylethylene (DPE) was rendered cationic by functionalization with a trimethylammonium bromide group. The synthesis route is shown in Figure 2. Hydroxybenzophenone was first reacted with 1,12-dibromododecane to form an ether linkage and then subjected to a Wittig reaction to convert the ketone into an ethylene functional group. Quaternization of the terminal –CH₂–Br functionality with trimethylamine resulted in the final product (trimethyl- $\{12-[4-(1\text{-phenylvinyl})\text{phenoxy}]\text{dodecyl}\}$ ammonium bromide) which was characterized by ¹H and ¹³C NMR spectroscopy. The detailed synthesis procedure and characterization are as follows:

Synthesis of 4-(12-Bromododecyloxy)benzophenone. 4-Hydroxybenzophenone (3.15 g, 15.9 mmol), 1,12-dibromododecane (5.22 g, 15.9 mmol), and potassium carbonate (2.76 g, 20 mmol) were charged into a one-neck flask with 40 mL of acetone. The mixture was refluxed overnight and then poured into water, extracted with ether, and dried over magnesium sulfate. After the solvent was evaporated, the residue was recrystallized from methanol to give 5.1 g of white crystals (yield

(10) Hadjichristidis, N.; Iatrou, H.; Pispas, S.; Pitsikalis, M. *J. Polym. Sci. A: Polym. Chem.* **2000**, *38*, 3211.

(11) Szwarc, M. *Nature* **1956**, *178*, 1168.

(12) Pitsikalis, M.; Pispas, S.; Mays, J.; Hadjichristidis, N. *Adv. Polym. Sci.* **1998**, *135*, 1.

(13) Alexandre, M.; Dubois, P. *Mater. Sci. Eng.* **2000**, *28*, 1.

(14) Szwarc, M. *Carbanions, Living Polymers and Electron-Transfer Processes*; Interscience: New York, 1968.

(15) Zhou, Q.; Fan, X.; Xia, C.; Mays, J.; Advincula, R. C. *Chem. Mater.* **2001**, *13*, 2465.

(16) Quirk, R.; Yoo, T.; Lee, Y.; Kim, J.; Lee, B. *Adv. Polym. Sci.* **2000**, *153*, 69.

65%). $^1\text{H NMR } \delta$ (ppm): 7.83 (dt, 2H), 7.76 (dt, 2H), 7.56 (tt, 1H), 7.47 (tt, 2H), 6.95 (dt, 2H), 4.04 (t, 2H), 3.41 (t, 2H), 1.83 (m, 4H), 1.47–1.29 (m, 16H). $^{13}\text{C NMR } \delta$ (ppm): 195.59, 162.87, 138.35, 132.58, 131.84, 129.88, 129.72, 128.17, 114.00, 68.27, 34.10, 32.82, 30.95, 29.52, 29.42, 29.35, 29.11, 28.76, 28.17, 25.99.

Synthesis of 4-(12-Bromododecyloxy)diphenylethylene.

To 4.94 mL of methyl lithium (1.4 M in hexane) was added to a dispersion of methyltriphenylphosphine bromide (2.00 g, 6.90 mmol) in 20 mL THF. The mixture was stirred for another hour after addition. A solution of 4-(12-bromododecyloxy)benzophenone (2.80 g, 6.3 mmol) in THF was then added dropwise to the mixture at -78°C . The reaction mixture was warmed to room temperature and stirred overnight. After workup, the mixture was poured into water, extracted with ether, and dried over magnesium sulfate, and the solvent was evaporated. The residue was recrystallized from methanol, which resulted in 1.74 g of colorless crystals (yield 63%). $^1\text{H NMR } \delta$ (ppm): 7.33 (m, 5H), 7.26 (dt, 2H), 6.85 (dt, 2H), 5.37 (dd, 2H), 3.97 (t, 2H), 3.41 (t, 2H), 1.82 (m, 4H), 1.46–1.28 (m, 16H). $^{13}\text{C NMR } \delta$ (ppm): 158.91, 149.54, 141.85, 133.72, 129.34, 128.33, 128.10, 127.62, 114.04, 112.84, 68.00, 34.10, 33.56, 32.83, 30.51, 29.53, 29.39, 29.28, 28.77, 28.54, 28.17, 26.05.

Synthesis of Trimethyl-[12-[4-(1-phenylvinyl)phenoxy]-dodecyl]ammonium Bromide. The organic cation was made by stirring 1.00 g (2.3 mmol) of 4-(12-bromododecyloxy)diphenylethylene and 20 mL of a 10% (w/w) trimethylamine solution in methanol for 3 days. After the solvent was evaporated, the residue was redissolved in cold methanol and filtered using a Buchner funnel. The filtrate was collected, and 1.0 g of product was obtained after the solvent was swept off (yield 86%). $^1\text{H NMR } \delta$ (ppm): 7.33(m, 5H), 7.26(d, 2H), 6.86(d, 2H), 5.34(d, 2H), 3.97(t, 2H), 3.58(p, 2H), 3.47(m, 9H), 1.77(m, 4H), 1.47–1.27(m, 16H) $^{13}\text{C NMR } \delta$ (ppm): 159.30, 142.23, 134.11, 129.75, 128.72, 128.51, 128.04, 114.45, 113.33, 68.40, 67.50, 53.81, 29.92, 29.88, 29.82, 29.78, 29.75, 29.68, 29.62, 29.55, 26.55, 26.45, 23.61.

Preparation of Intercalated Clay. One gram of montmorillonite clay was dispersed in 500 mL of deionized water and stirred vigorously overnight at room temperature. The clay suspension was then ultrasonicated with stirring for 24 h until a yellowish, homogeneous dispersion was obtained.¹⁷ The size and dimension of nanoparticle clay in the homogenized suspension are in the form of partially exfoliated platelets according to the AFM results (see Figure 9). These nanoparticles were used for LASIP in contrast to previous procedures, which involved intercalation of the initiator to bulk montmorillonite clay particles by the formation of organic layered silicates (OLSs).^{3c}

The DPE initiator was dissolved in deionized water to make 1.25% (w/w) aqueous solution. By using the cation-exchange capacity (CEC) value (92 mequiv/100 g) of Cloisite Na⁺ and the molecular weight (MW) of the initiator, the exact weight (the weight of the initiator needed to fully replace the Na⁺ of the clay) of the initiator to be used was calculated. A 10% excess of initiator solution was slowly poured into the clay dispersion while it was being stirred and ultrasonicated. The mixture was then stirred and ultrasonicated for another 24 h. The resulting white precipitate was separated by filtration and redissolved in deionized water. This filtration–dissolution process was repeated ten times to remove the free, unattached initiator. The final product was weighed after the precipitate had been dried in a vacuum oven for 3 days, and the reaction yield was calculated. The yellowish powder product was stored in a desiccator for further characterization and subsequent use in living anionic SIP. Table 1 summarizes the gravimetric results for the preparation of the intercalated clay.

Polymerization Setup and Procedure. A schematic diagram of the vacuum polymerization apparatus is shown in Figure 3. The sequence of the polymerization procedure is as follows: After the DPE initiator–intercalated clay nanoparticles had been added to the reactor, the system was connected to the vacuum line, and the reactor was heated to 120°C for at least 8 h and then cooled. An excess amount of *n*-BuLi in benzene solution was then added to the intercalated clay, followed by extensive washing and filtration in vacuo to remove extra *n*-BuLi and any

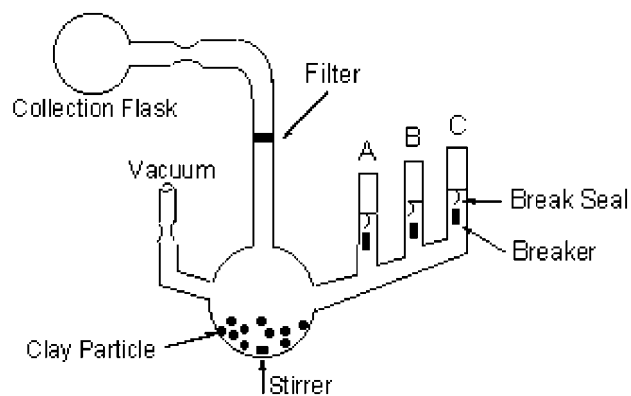


Figure 3. Schematic diagram of the anionic polymerization reactor: (A) ampule containing styrene, (B) ampule containing *n*-BuLi, (C) ampule containing MeOH.

Table 1. Results of the Preparation of Intercalated Clay

weight of clay used	exact initiator weight	weight of initiator actually added	weight of intercalated clay obtained	yield
1 g	0.462 g	0.516 g	1.20 g	79%

unattached DPE initiator. Afterward, styrene monomer in benzene solution was added, and the polymerization was continued up to 8 h. Finally, the reaction was terminated by the addition of MeOH. The filtration unit in the reactor facilitated transfer of solvent between washings while leaving the particles in the reaction vessel.

Polymer Separation. After several washing procedures with toluene to remove any free polymer (polymer formed from any unbound initiator or *n*-BuLi), the remaining polymer bound on the clay was cleaved off by refluxing the polymer–clay nanocomposite with LiBr in tetrahydrofuran (THF) with stirring. The cleaved polymers were separated from the solid clay nanoparticles by centrifugation. NMR, FT-IR, size-exclusion chromatography, and thermogravimetric analyses were performed on the polymer–clay nanocomposite and the detached polymer.

Characterization and Instrumentation. ^1H and ^{13}C NMR spectra were obtained on a Bruker ARX-300 spectrometer using chloroform-*d* as the solvent and tetramethylsilane as the internal reference.

X-ray diffraction (XRD) analysis of powder samples was performed on a Philips X'pert PW3040-MPD model diffractometer with a Cu K α incident beam of wavelength 0.1543 nm. The Bragg equation was applied to calculate the *d* spacing of the clay samples.

Thermogravimetric analysis (TGA) was performed on a Mettler TGA50/DSC30 instrument at a heating rate of $20^\circ\text{C}/\text{min}$. All measurements were performed under airflow. All samples were in a dried powder state and were measured as they were synthesized. No further drying treatment was applied before the TGA measurement.

X-ray photoelectron spectroscopy (XPS) of the pure and intercalated clays was performed using a Kratos Axis 165 multitechnique electron spectrometer system. Powder samples were first pressed onto double-sided inert carbon tape before being loaded into the XPS analysis chamber. A nonmonochromatic Al K α X-ray source (1486.6 eV) operated at 15 kV and 20 mA was applied to excite the photoelectron emission. Fixed analyzer transmission (FAT) mode was used and survey scans (spot of area $800 \times 200 \mu\text{m}^2$ with a resolution of 4 eV at an analyzer pass energy of 160 eV) were collected from 0 to 1400 eV to obtain the elemental compositions of the powder samples. The C 1s peak of hydrocarbon signal (284.5 eV) was used as the binding energy reference. A built-in charge neutralizer was operated to compensate for charge buildup during the measurements.

Size-exclusion chromatography (SEC) with polystyrene standards was used to determine the molecular weights and polydispersity indices of the free polystyrene formed in solution and the polystyrene attached to clay surface.

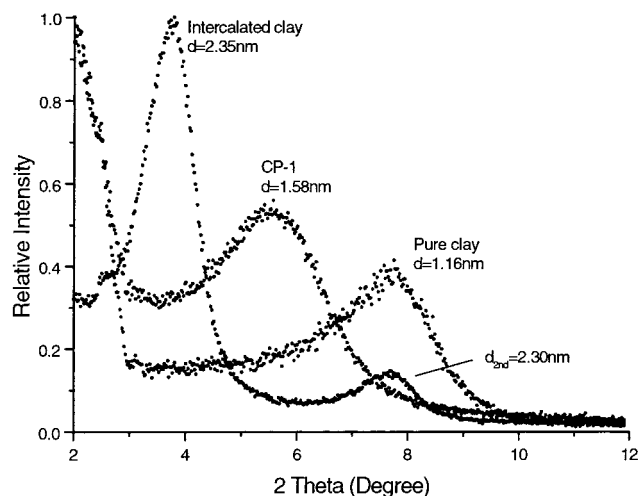


Figure 4. X-ray diffractogram of montmorillonite clay samples, with the initiator and after polymerization.

Infrared (IR) spectra were recorded on a Nicolet NEXUS 470 FT-IR system. Powder samples were dispersed in anhydrous $\text{CH}_2\text{-Cl}_2$ and drops of the liquid were spread on KBr plates. All sample disks were fully dried in air before analysis. The spectra were scanned 64 times with a resolution of 4 cm^{-1} .

For atomic force microscopy (AFM) of the samples, pristine montmorillonite clay was dispersed in water, and clay-polystyrene composite (after refluxing separation) was dispersed in toluene. Both 1% (w/w) dispersions were spin-coated onto silicon wafers at 2000 rpm for 90 s, and their AFM micrographs were recorded. The clay particle morphologies before and after SIP were studied using a PicoScan system (Molecular Imaging) equipped with an $8 \times 8\ \mu\text{m}^2$ scanner. Magnetic AC (MAC) mode was used for all AFM images. A MAC lever, i.e., a silicon-nitride-based cantilever coated with magnetic film, was used as the AFM tip. The force constant of the tip was 0.5 N/m, and the resonance frequency was around 100 kHz. All samples were measured inside a suspension chamber to minimize ambient disturbance.

Results and Discussion

Structural Characterization of the DPE Derivative. Both ^1H and ^{13}C NMR analyses indicate that the target molecule, trimethyl- $\{12\text{-}[4\text{-}(1\text{-phenylvinyl})\text{phenoxy}]\text{dodecyl}\}$ ammonium bromide, was indeed successfully synthesized, as shown in Figure 2. The important ^1H and ^{13}C NMR peaks are summarized in the Experimental Section. An important property of the synthesized initiator is its solubility as a surfactant. A solution of the initiator in deionized water was successfully prepared and introduced with the dispersed clay nanoparticles for cation exchange. The cation exchange of the initiator was confirmed by X-ray, IR, XPS, and TGA methods.

Characterization of Intercalated Clay. X-ray powder diffraction patterns of pristine clay and intercalated clay are shown in Figure 4. Using the Bragg equation, $n\lambda = 2d\sin\theta$, the d spacing values between layers of the clay lamellae were calculated. The DPE initiator was successfully intercalated into the galleries of the partially exfoliated clay nanoparticles. The d spacing increased from 1.16 nm for the pristine clay to 2.35 nm for the initiator-intercalated clay. By subtracting the 0.9-nm thickness of a single montmorillonite lamellar layer,¹⁷ the distance between two adjacent clay layers after intercalation is determined to be 1.45 nm. Vaia et al. reported a value of 1.43 nm as the gallery height of montmorillonite clay layers intercalated by an organic surfactant molecule with a $\text{C}_{18}\text{H}_{37}$ alkyl tail and a quaternized amine end group.¹⁸

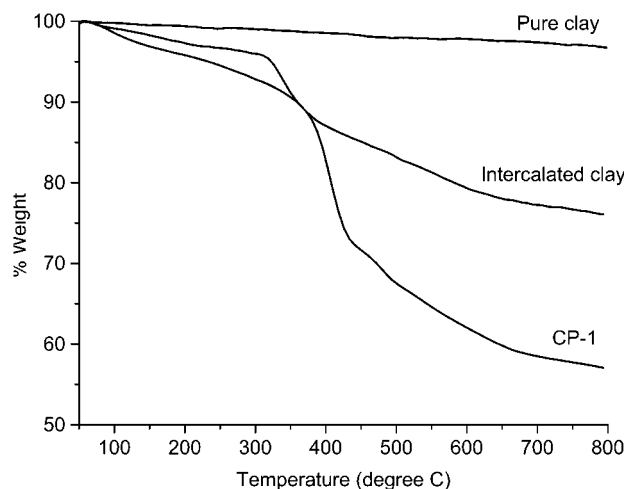


Figure 5. TGA traces of montmorillonite clay samples, with the initiator, and after polymerization.

The lateral lengths (estimated by Chem 3D software) of the two molecules are similar: 2.55 nm for DPE and 2.41 nm for the other organic molecule, indicating consistency of the intercalated molecules' dimensions. Furthermore, the increased diffraction intensity is also evidence of a well-ordered structure after intercalation. These results demonstrate that the lamellae of inorganic clays can easily accommodate the modified DPE initiator with long-range periodicities. Interestingly, for the intercalated clay, another low-intensity peak was observed at 7.7° (2θ) in addition to the high-intensity peak at 3.8° . There are two possibilities for this second peak: (1) It might be the second-order, $n = 2$, diffraction peak with d spacing = 2.3 nm, which is very close to the value of its first-order diffraction peak. (2) It might also originate from the remaining, unintercalated clay particles because the position of this peak coincides with that of pristine clay. Nevertheless, this is a very small portion of the sample because the intensity of this peak is much smaller than the first one. This second possibility was ruled out, however, by TGA and XPS analysis as discussed later. The XRD curve and the d spacing values of the product CP-1 after SIP in Figure 4 are also explained in a later discussion.

Figure 5 shows the TGA traces of pure clay, intercalated clay, and sample CP-1 (after removal of free polymer). As expected, the inorganic montmorillonite silicate showed a very high thermal stability. The total weight loss even at 800°C was only 2.5%. This small percentage is due to the three different types of water present in montmorillonite clay.¹⁹ Also, judging from the figure, the intercalated clay has two significant decomposition processes, one major weight loss at approximately $250\text{--}350^\circ\text{C}$ and another minor weight loss at about $400\text{--}600^\circ\text{C}$. The first decomposition is due to breakdown of the DPE unit. The second degradation is consistent with the decomposition of the alkyl spacer or whole molecule. This clearly indicates the attachment of the organic initiators to the inorganic nanoparticle clay surface and interface. By using the CEC value, the ideal organic weight percentage for the intercalated clay was calculated to be 25%. The observed weight loss by TGA was 26%. This consistency between calculated and experimental data indicates a nearly complete cation-exchange process, suggesting that the host gallery spaces were indeed swollen by the guest-charged DPE derivative

(18) Vaia, R. A.; Teukolsky, K. R.; Giannelis, E. P. *Chem. Mater.* **1994**, *6*, 1017.

(19) Xie, W.; Gao, Z.; Pan, W.; Hunter, Vaia, R.; Singh, D. A. *PMSE Prepr.* **2000**, *82*, 284.

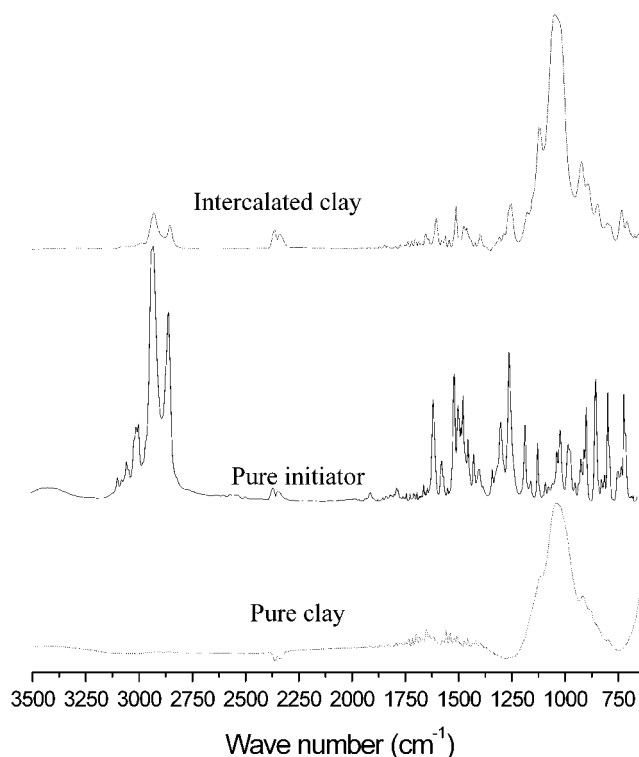


Figure 6. FT-IR spectra of pure clay, pure initiator, and intercalated clay.

through the intercalation procedure. A similar TGA result was observed in the case of intercalation of a living free-radical polymerization (LFRP) initiator into montmorillonite clay.^{3a} A small amount of free unattached initiator that was not completely washed away cannot be discounted. Figure 5 also shows the bound polymer on clay as it decomposed at about 418 °C, which is typical of the decomposition temperature of polystyrene. The TGA weight loss of this sample was around 62%. These measurements were done in air. The slow thermal decay below 200 °C is typical of all of the initiator–clay and polymer–clay samples that were exposed to ambient temperature and humidity conditions prior to the TGA experiment.

IR analysis further confirmed the presence of the organic initiator in the intercalated clay. In Figure 6, the IR spectrum of pure clay shows only a strong absorbance at about 1040 cm^{-1} due to the Si–O–Si bond in montmorillonite silicate. The spectrum of the pure initiator shows strong characteristic peaks at 3100–2800 cm^{-1} due to aromatic and aliphatic C–H stretching, 1475–1300 cm^{-1} due to alkyl C–H bending, and 1675–1550 cm^{-1} due to aromatic and aliphatic C=C stretching. Also, peaks within the range of 1520–1480 cm^{-1} can be attributed to C–N bond deformation, and peaks near 1250 cm^{-1} to alkyl C–C stretching. The above peaks of pure silicate and pure initiator can easily be found in the same frequency regions in the IR spectrum of the intercalated clay, which is clearly an overlapping combination of the two spectra. This demonstrates clearly the attachment of the DPE derivative onto the clay surface. Similar IR results for this synergistic effect on organic modified clays were observed in poly-aniline–montmorillonite and styrene–acrylonitrile–montmorillonite systems.^{20,21}

(20) Choi, J.; Kim, W.; Kim, G.; Kim, H.; Joo, J. *PMSE Prepr.* **2000**, *82*, 245.

(21) Choi, J.; Kim, W.; Jhon, *MPMSE Prepr.* **2000**, *82*, 247.

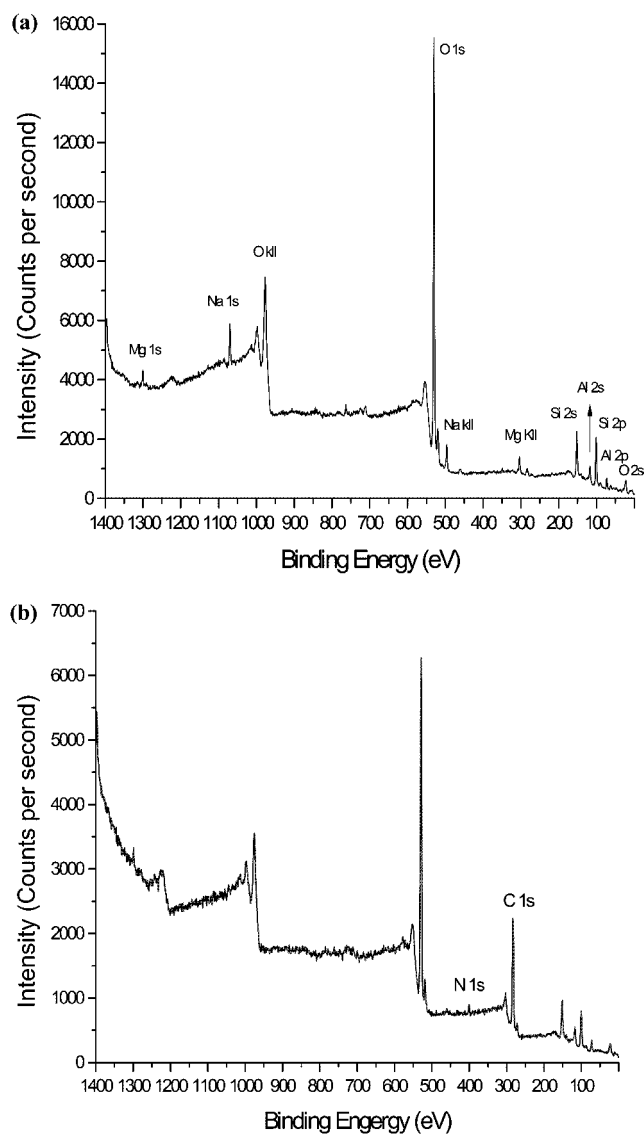
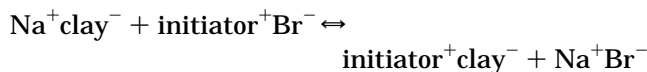


Figure 7. XPS spectra of (a) pure and (b) intercalated clay.

The cation-exchange process of Na^+ montmorillonite clay and charged initiator can be simply expressed by the reaction



If all of the Na^+ ions are replaced by initiator cations and the product is thoroughly washed, no Na^+ ions should remain in the intercalated clay. By using XPS, the complete ion-exchange reaction was confirmed. Figure 7a and b shows the XPS survey scan spectra of the pure and intercalated clay samples. Characteristic peaks of O, Si, Al, Mg, and Na are very clear for montmorillonite clay, which is chemically a type of magnesium aluminum silicate. In addition to these signals from clay, the right spectrum also shows the C 1s and N 1s peaks, confirming the presence of the organic initiator molecules on the clay. However, the most important result from XPS analysis is the change in Na signal before and after ion exchange. In the above spectrum, the photoelectron line of Na 1s (1072 eV) and the Auger line of Na KLL (493 eV) are very prominent, indicating that the clay's counterion is made up of Na^+ . After the cation-exchange process, those two characteristic peaks for Na disappear as shown in Figure

Table 2. Summary of SEC Results for Anionic Polymerization of Styrene on Clay Surfaces

sample	styrene/DPE (g/mmol)	M_n (SEC) ^a × 10 ⁻³ (s) ^b	PDI ^c (s) ^b	M_n (SEC) ^a × 10 ⁻³ (c) ^d	PDI ^c (c) ^d	bound PS/clay (PS/g of clay) (g)
CP-1	14.6	78.6	1.09	11.9	1.44	0.62
CP-6	19.9	58.5	1.30	21.8	1.30	0.81
CP-3	9.6	35.5	1.20	7.4	1.31	0.45
CP-4 ^e	21.8	100.1	1.10	23.6	1.40	0.79

^a Number-average molecular weight (M_n) and weight-average molecular weight (M_w) were determined by SEC with PS standard. ^b Polymer formed in solution. ^c Polydispersity index, M_w/M_n . ^d Polymer cleaved from clay surfaces. ^e Cumyl potassium used as initiator instead of *n*-BuLi.

7b. Other than the TGA result, this is confirming evidence supporting our conclusion of a nearly complete cation-exchange process. Thus, the second XRD peak previously discussed should be considered as second-order diffraction from the totally intercalated clay lamellae, rather than signal from a remaining small portion of unintercalated clay particles.

LASIP Reaction. Room temperature as well as high vacuum was not enough to remove trace impurities such as H₂O, which can result in a broadened MW distribution.²² We found that the successful polymerization of styrene from clay nanoparticles was realized only by using a higher temperature and high vacuum. Previous TGA thermograms did not show any significant decomposition of the DPE derivative below 200 °C, which is an advantage of DPE as an initiator because the high temperature of 120 °C could be used to dry intercalated clay completely. This ensured that the initiator–clay is free of any trapped H₂O that can terminate a living anion.

Excess *n*-BuLi must be used for efficient activation of DPE and reaction with any bound –OH groups. Another reason is that BuLi tends to form aggregates in benzene solvent.

As shown in Figure 3, the SIP reaction was carried out under high vacuum in a specially designed reactor with a built-in filter to allow for the separation of clay from excess initiator during each washing step. Because *n*-BuLi activates DPE very slowly in hydrocarbon solvents, we paid careful attention to the reaction period. Following the activation of DPE, a red color was observed when the solvent was poured into the collection flask to remove excess *n*-BuLi. This color is attributed to the formation of a Li–DPE anion complex, commonly observed with the DPE initiator.¹⁶ A second wash resulted in a colorless or a pale yellow solvent in the collection bottle, with the red solid clay staying on the filter. These color changes indicate that some unattached initiator still remained even after repeated dissolution and centrifugation of DPE-intercalated clay. Eventually, only the clay particles (suspension) exhibited the red color after several washings with solvent and filtrations.

It is essential that free BuLi be removed because it competes with the tethered initiator for monomers and strongly affects the reproducibility of the polymerization (unpredictable MW). It is also worth noting that the filter unit in the reactor made it possible to investigate the effect of free, unattached initiator in the system. Nevertheless, a small amount of polymer still formed in solution either from unremoved *n*-BuLi or from unattached DPE initiators (Table 2). No significant differences in results were observed when the larger cumyl potassium (instead of *n*-BuLi) was used to activate DPE (CP-4 in Table 2). This fact led us to conclude that no significant cation exchange could be attributed to Li⁺ after the decomposition of BuLi or its aggregates.

LASIP-Attached Polystyrene Product Analysis.

SEC analysis of the free polymer (formed in solution) and detached clay-bound polymer (formed on the clay surface) from four batches of LASIP products are summarized in Table 2. A linear correlation between monomer concentration (grams per millimole) and M_n for the cleaved polymers, CP-3 < CP-1 < CP-6, indicated a living anionic polymerization mechanism.¹¹ Polymers initiated by a free initiator in solution have a very narrow molecular weight distribution. This shows that styrene was polymerized via the living anionic mechanism in solution and that the quaternized amine end group introduced no side reactions to anionic polymerization. This is another positive attribute for using DPE as the initiator. The bound polymer had a much lower MW and broader distribution or polydispersity index (PDI) than polymer formed in solution. Wittmer previously reported that living anionic polymerization at surfaces does not necessarily promote simultaneously growing living chain ends that should result in a Poisson type of MW distribution.²⁴ This is due to entropic difficulties associated with the transport or diffusion of monomers at the surface and conformational requirements of a growing polymer chain. In contrast, a narrow MW distribution is the typical case for polymers prepared by the living anionic polymerization in solution.¹⁴ We also recently observed a broadened MW distribution with LASIP prepared on spherical Si nanoparticles.²⁵

Three other factors can contribute to a broadened MW distribution: nanoparticle aggregation, inefficiency of intergallery initiation, and polymerization by *n*-BuLi or unbound DPE. The first can be attributed to formation of clay nanoparticle aggregates in solution, which tend to reduce initiator activation efficiency and subsequent polymerization.²⁵ A consequence of this is a reduced number of initiators available on the surface of the nanoparticles. In the case of lamella-bound initiators, a tight intergallery spacing (1.45 nm in this case) between clay platelets might prohibit the styrene monomer from reaching DPE initiator sites in the interlayers when the monomer is added.³ Akelah et al. reported the effect of the initial amount of styrene inserted into the interlayers on the intercalation of a growing polymer.²³ In principle, the polymer can grow only within the clay lamellae when monomer diffuses inside the interlayers and is initiated by the activated surfaces.³ However, the kinetics of monomer diffusion is much slower than that of the reaction between monomer and initiator. Thus, living anions outside tend to exhaust most of the monomers in solution. Consistent with the findings by Wittmer et al.,²⁴ the initially formed longer chains, whether at the surface or at the lamellar interface, will compete more effectively for monomer than shorter chains, resulting in a broadened

(23) Akelah, A.; Moet, A. *J. Mater. Sci.* **1996**, *31*, 3589.

(24) Wittmer, J.; Cates, M.; Johner, A.; Turner, M. *Europhys. Lett.* **1996**, *33*, 397.

(25) Advincula, R.; Zhou, Q.; Wang, S.; Fan, X.; Mays, J. Living Anionic Surface-Initiated Polymerization (LASIP) of a Polymer on Silica Nanoparticles. *Langmuir* **2002**, *18* (8), 3324–3331.

(22) Oosterling, M. L. C. M.; Sein, A.; Schouten, A. J. *Polymer* **1992**, *20*, 4394.

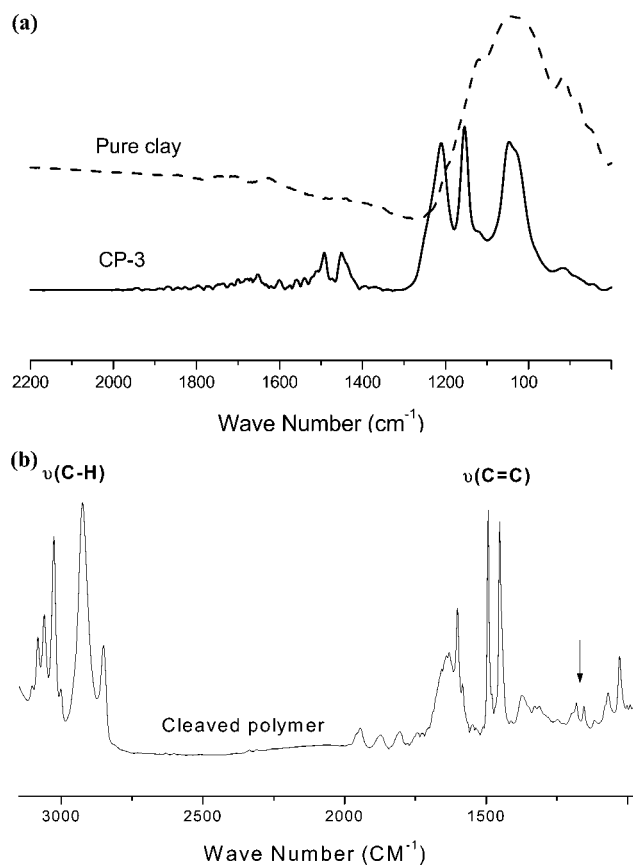


Figure 8. (a) IR spectra of pure clay and polystyrene-bound clay. (b) IR spectrum of cleaved polystyrene.

molecular weight distribution. The last possibility, that of polymers formed by initiation with *n*-BuLi and unbound DPE, can be largely minimized by exhaustive removal of any unbound polymer that is physically adsorbed (not electrostatically bound) using Soxhlet extraction techniques.

We believe that monomer accessibility to DPE anionic sites is the key element toward improving future procedures, that is, to make the clay *fully intercalated* (maximum *d* spacing) and *dispersed* as single particles in the polymerization solvent. Clearly, further experiments are needed to distinguish these factors for efficient LASIP procedures. Nevertheless, this current procedure affords the preparation of a truly in situ polymerized nanocomposite material.

IR analysis confirmed the presence of the polymer on clay. As shown in Figure 8a, the spectrum of sample CP-3 (after free polymer removal) shows C=C double bond stretching vibrations at 1600, 1549, and 1458 cm^{-1} compared to the spectrum of pure clay, which has only a broad peak centered at 1050 cm^{-1} (Si-O-Si asymmetric stretching). Also in Figure 8a, prominent peaks around 1200 cm^{-1} , which did not exist with pure clay, are attributed to the C-N-C asymmetric stretch of the $-\text{C}(\text{CH}_3)_3\text{N}^+\text{Br}^-$ end group. These peaks can also be seen (indicated by an arrow in Figure 8b) in the spectrum of the detached polystyrene, albeit at much lower intensity. This indicates that the polymer chain was bound to the clay surface through the DPE derivative by electrostatic attraction. In Figure 8b, the vibrational bands typical for polystyrene, such as the C-H stretching vibrations around 3000 cm^{-1} , were also observed. Moreover, the ^1H NMR spectrum of the cleaved polymer showed the broadened proton signal of the styrene phenyl ring at 7.04 ppm, CH_2 protons at 1.28 ppm, and protons of the trimethyl group

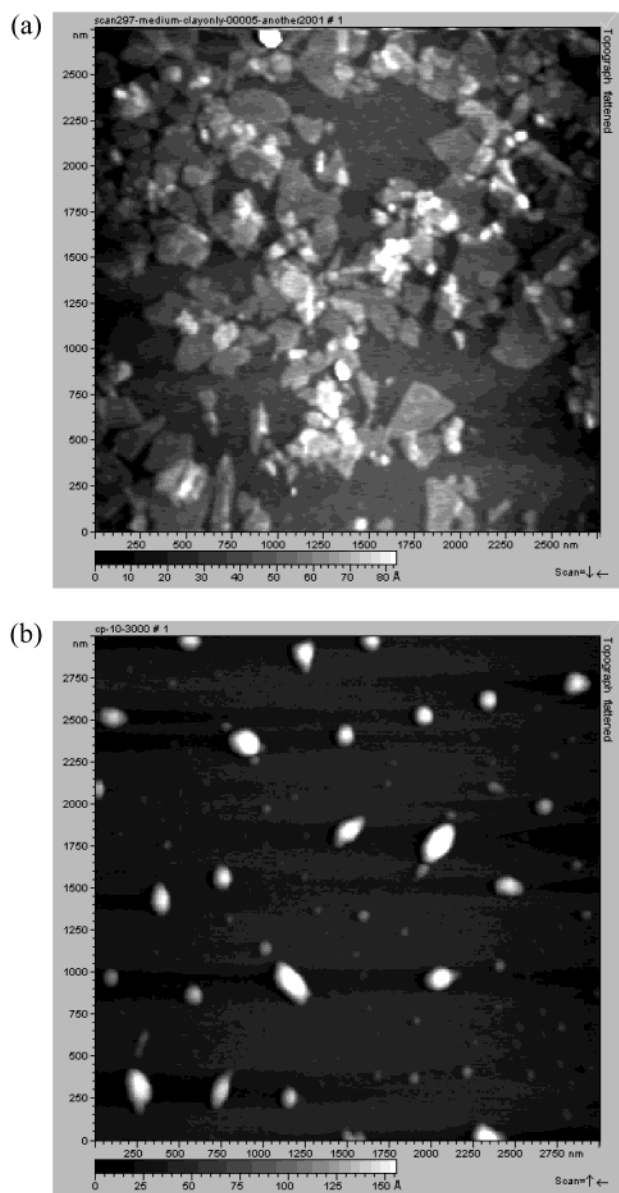


Figure 9. AFM images of (a) pure clay and (b) clay particle morphology after SIP.

at 3.38 ppm. Thus, these spectroscopic results further confirm that the polymerization was not affected by the ionically modified DPE derivative.

From the TGA data, the weight percentage of bound polymer to clay (TGA decomposition) or PS/g of clay (last column in Table 2) is lower than the theoretical value calculated for clay surfaces.^{3a} We believe that this is further indication of the low initiation/monomer addition efficiency. Together with the low MW and higher polydispersity observed for the detached polymers, one can conclude that most of the initiation occurred at the surface of the clay rather than at the intergallery spaces of the clay lamellae.³ This is further supported by XRD in which the polymer-clay composite showed a *d* spacing based on a very broad peak centered at 1.58 nm, which is between the values for pure clay and intercalated clay (Figure 4). These results are clearly different from the previous report using LFRP.^{3a} Primarily, the high surface initiation/polymerization is also a consequence of using dispersed and partially exfoliated montmorillonite clay nanoparticles¹⁷ rather than bulk particles, which have more intergallery interfacial volume.

Our AFM observations showed partially exfoliated clay nanoparticle platelets that were $\sim 1\text{--}5$ nm in thickness and a very wide diameter distribution from ~ 35 to 300 nm (Figure 9a) were obtained after the stirring–ultrasonication process. The images were taken after a drop of a dilute solution of the nanoparticles was placed on a clean Si wafer and allowed to dry. The edges are well-defined with high aspect ratios compared to silicate spherical nanoparticles.²⁵ After polymerization, the polymer-bound clay nanoparticles showed very smooth edges compared to the initial platelets' sharp edges (Figure 9b). Also, the particles did not exhibit good adhesion to the Si wafer and were more three-dimensional in orientation, appearing smaller. This indicates that a range of exfoliated and unexfoliated particles made up the original clay samples. This result is consistent with the XRD measurements. A large part of the intercalated initiator inside the clay lamellae was not activated for anionic polymerization, with significant initiation taking place only at the outer surface (perimeter) of the intercalated clay. Comparable results have been observed with LASIP on silica nanoparticles.²⁵ Future studies will be focused on determining the mechanism of LASIP through model studies and the feasibility of block copolymerization.

Conclusions

A charged diphenylethylene (DPE) initiator derivative for living anionic surface-initiated polymerization (LASIP) was successfully synthesized. Its intercalation into montmorillonite clay nanoparticles was confirmed. XRD results showed that the d spacing increased from 1.14 nm for original clay to 2.35 nm for intercalated clay. IR, TGA, and XPS results also confirmed the attachment of the initiator at the interface. Moreover, complete replacement

of clay Na^+ ions by charged initiators was demonstrated by TGA and XPS. The simple stirring–ultrasonication process at room temperature achieves successful intercalation and complete ion exchange of montmorillonite clay. The initiation process and molecular weight data indicate that SIP was realized in a living anionic mechanism. IR and TGA confirmed the attachment of polystyrene from clay surfaces for the nanocomposite material. However, polymer bound to the clay surface had a lower MW and a higher MW distribution (polydispersity index, PDI) than free polymers formed in solution. By TGA, XRD, and AFM, it was found that the initiation/chain growth efficiency inside clay interlayer spaces was lower than that of clay perimeter surfaces. This work clearly demonstrates the preparation of polymer–clay nanocomposites using LASIP. A full understanding of the mechanism and control of polymerization efficiency will allow for the preparation of bulk materials that can be tested for their physical and mechanical properties.

Acknowledgment. This project is supported by the Army Research Office (Grant DAAD-19-99-1-0106). Discussions with co-workers at the Army Research Lab (Aberden Proving Grounds, MD) are gratefully appreciated. Montmorillonite clay (commercial Cloisite Na^+) was generously provided by Southern Clay Products (Gonzales, TX). The authors appreciate Dr. Yogesh Vohra, Dr. Shane Catledge, Dr. Juan Pablo Claude, and John Kestell at University of Alabama at Birmingham for access to XRD and IR instrumentation. The assistance of Dr. Earl Ada at University of Alabama-Tuscaloosa for XPS measurements is also acknowledged.

LA025556+